Impact of the shape of the acquisition surface on the effectiveness of the ISS internal multiple attenuation and elimination algorithms: analyzing the problem and providing a response to the challenge

Yuchang Shen and Arthur Weglein, M-OSRP, University of Houston

SUMMARY

The inverse scattering series (ISS) internal multiple attenuation and elimination algorithms have the stand-alone capability for multiple removal, because they do not require subsurface information. The ISS internal multiple attenuation algorithm, proposed by Araujo et al. (1994), Weglein et al. (1997) and Weglein et al. (2003), can predict the exact time and approximate amplitude of all first-order internal multiples without subsurface information. In order to extend the capability of the attenuation algorithm, Y. Zou et al. (2016) proposed the ISS internal multiple elimination algorithm, that can predict the exact time and amplitude of all first-order internal multiples without subsurface information. Both the current published form of the multiple-attenuation algorithm and elimination algorithm are derived from the inverse-scattering series, and assume a horizontal acquisition surface. When the acquisition surface is non-horizontal, for example as often can occur in an ocean-bottom survey and with an on-shore play, if we treat the non-horizontal acquisition surface as if it is horizontal, the current form of internal multiple attenuation and elimination algorithms will give severe artifacts in their prediction results. In this paper we (1) provide a detailed explanation and analysis for the origin of those artifacts and (2) develop and illustrate a new method that avoids the horizontal acquisition assumption and the artifacts that arise when that assumption is violated.

INTRODUCTION

As one of the seismic processing objectives that can be accommodated by the inverse-scattering series, the ISS internal multiple attenuation algorithm can predict the correct time and approximate amplitude of all first-order internal multiples generated from all reflectors without any subsurface information. When the internal multiples are isolated from the target primaries, the approximate amplitude of the predicted multiples can be fixed by energy-minimization adaptive subtraction, which can lead to the elimination of internal multiples. But when the multiples are interfering with the primaries, the energy-minimization criteria may fail, and the internal multiple elimination task becomes challenging. As a response to this challenge, Y. Zou et al. (2014), Y. Zou et al. (2016) develop the ISS internal multiple elimination algorithm based on the previous attenuation algorithm, which can in principle eliminate all first-order internal multiples without any subsurface information, and without the energy-minimization adaptive subtraction. Despite the unique strength provided by the ISS internal multiple elimination algorithm, the method does have certain prerequisites and assumptions. The ISS internal multiple attenuation algorithm and elimination algorithm require the removal of (1) the reference wave, (2) both source and receiver side ghosts, and (3) the free-surface multiples from the input data, prior to the application of the method. On the other hand, the algorithm is derived from the inverse-scattering series with the assumption that the data are acquired on a horizontal acquisition surface. In certain scenarios, however, this assumption can be violated as in the feathering of a marine towed streamer, ocean-bottom acquisition, or on-shore acquisition. Both cases involve non-horizontal acquisition surfaces, which may bring in severe artifacts to the internal multiple predictions, both in time and amplitude. In this paper, we investigate the impact of the shape of the acquisition surface on the ISS internal multiple attenuation and elimination algorithms by treating a non-horizontal acquisition surface as if it is horizontal, and we propose a solution based on Green's theorem wave-field prediction to fix the negative impact on the multiple prediction results due to wrong assumption of the acquisition surface. The variation of the depth of the acquisition surface is made to be larger than expected in actual seismic data acquisition to show the impact of the wrong assumption and the effectiveness of the method.

ISS INTERNAL MULTIPLE ATTENUATION AND ELIMINATION ALGORITHM

The ISS internal multiple attenuation algorithm was first derived by Araujo et al. (1994) and Weglein et al. (1997). The 1D normal-incident version of the algorithm is the following

$$b_3^{IM}(k) = \int_{-\infty}^{+\infty} dz e^{ikz} b_1(z) \int_{-\infty}^{z-\varepsilon_2} dz' e^{-ikz'} b_1(z') \int_{z'+\varepsilon_1}^{\infty} dz'' e^{ikz''} b_1(z'') \quad (1)$$

In equation 1, $b_1(z)$ is the constant-velocity Stolt migration of a 1D normal-incident spike plane wave. $b_3^{IM}(k)$ is the predicted first-order internal multiples in the vertical wavenumber domain. The 2D version of the algorithm was also derived and developed in Araujo et al. (1994), Weglein et al. (1997), and Weglein et al. (2003). The 3D version is a straightforward extension. The ISS internal multiple attenuation algorithm combines three primary events in the data to predict one first-order internal multiple. The mechanism for predicting a first-order internal multiple generated by the first reflector is demonstrated in figure 1 (Y. Zou et al. (2016)). Each one of the three primaries has their own traveling history which carries different combinations of transmission coefficients and reflection coefficients. When these three primaries serve as the sub-events to predict the internal multiple, they carry their own coefficients into the algorithm and introduce some extra transmission coefficients to the amplitude of the predicted multiple (Weglein et al. (2003)). The amplitude of the attenuation prediction by equation 1 is the amplitude of the actual multiple times the product of all transmission coefficients down to the shallowest reflector where the internal multiple experiences a downward reflection. For the first-order internal multiple generated by the first reflector, the difference between the amplitude of the actual and predicted multiple will be $-T_{01}T_{10}$. In order to

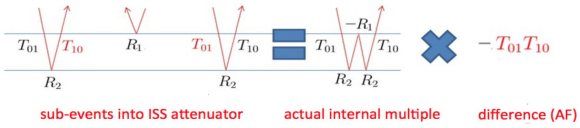

Figure 1: An example of the attenuation factor of a first-order internal multiple generated at the shallowest reflector; notice that all red terms are extra transmission coefficients (Y. Zou et al. (2016)).

overcome the difference between the amplitude of the actual inter-

nal multiple and the predicted internal multiple, Y. Zou et al. (2014) developed an elimination algorithm that can in principle eliminate all first-order internal multiple for a 1D earth.

$$b_E(k,2q) = \int_{-\infty}^{+\infty} dz e^{2iqz} b_1(k,z) \int_{-\infty}^{z-\varepsilon_1} dz' e^{-2iqz'} F[b_1(k,z')] \times \int_{z'+\varepsilon_2}^{+\infty} dz'' e^{2iqz''} b_1(k,z'') \quad (2)$$

$$F[b_1(k,z')] = \frac{1}{2\pi} \int_{-\infty}^{+\infty} \int_{-\infty}^{+\infty} dz' dq' \times \frac{e^{-iq'z} e^{iq'z'} b_1(k,z')}{\left[1 - \int_{-\infty}^{z'-\varepsilon} dz'' b_1(k,z'') e^{iq'z''} \int_{z''-\varepsilon}^{z''+\varepsilon} dz''' g(k,z''') e^{-iq'z'''}\right]^2} \times \frac{1}{1 - \left|\int_{z'-\varepsilon}^{z'+\varepsilon} dz'' g(k,z'') e^{iqz''}\right|^2} \quad (3)$$

$$g(k,z) = \frac{1}{2\pi} \int_{-\infty}^{+\infty} \int_{-\infty}^{+\infty} dz' dq' \times \frac{e^{-iq'z} e^{iq'z'} b_1(k,z')}{1 - \int_{-\infty}^{z'-\varepsilon} dz'' b_1(k,z'') e^{1q'z''} \int_{z''-\varepsilon}^{z''+\varepsilon} dz''' g(k,z''') e^{-iq'z'''}} \quad (4)$$

In equation 2, 3, and 4, b_1 is the water-speed uncollapsed Stolt migration of the input data, b_E is the elimination prediction of the multiple in wavenumber domain, and F and g are two intermediate functions that fill the gap between the amplitude of the attenuation prediction and the actual multiple. These two intermediate functions are determind directly in terms of b_1 and without subsurface information. Figure 3 shows the numerical results of both the ISS internal multiple attenuation and elimination algorithm on a synthetic data set. The data are collected by a horizontal acquisition from a two-layered 1D earth model with two reflectors, shown by figure 2. The input data is generated analytically by the reflectivity method. We assume that the reference waves, the ghosts and the free-surface multiples are removed before the experiment by removing the free-surface from the model, and only the first-order internal multiple is considered in this case. So there are only three events in the input data, the primary from the first reflector, the primary from the second reflector, and the first-order internal multiple, shown as figure 3a (all the input data in this paper for different experiments are generated from the same earth model). Figure 3b shows the attenuation prediction, and figure 3c shows the elimination prediction. Figure 3d shows the trace comparison at offset 600m of the input data (blue), the attenuation prediction (red), and the elimination prediction (yellow), focusing on the internal multiple part. We can see that, when the acquisition surface is horizontal, which meets the assumption of the algorithm, the ISS internal multiple attenuation algorithm gives the correct time and approximate amplitude of the first-order internal multiple, while the elimination gives both correct time and amplitude of the multiple.

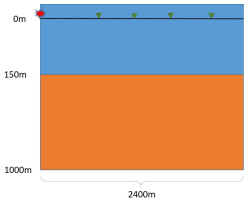

Figure 2: Earth model for the input data with a horizontal acquisition

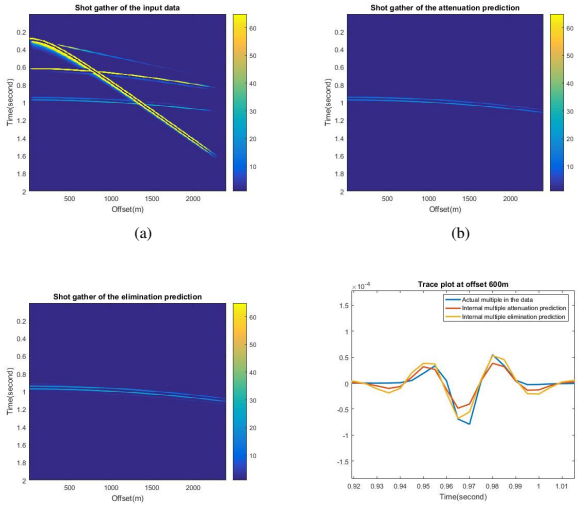

Figure 3: **(a)** Shot gather of the input data from a horizontal acquisition. **(b)** Shot gather of the attenuation prediction using figure 3a as input. **(c)** Shot gather of the elimination prediction using figure 3a as input. **(d)** Trace comparison at offset 600m.

IMPACT OF THE WRONG GEOMETRY ASSUMPTION ON THE ISS INTERNAL MULTIPLE ATTENUATION AND ELIMINATION ALGORITHM

As we discussed earlier in this paper, the assumption of a horizontal acquisition surface may not be satisfied at all times, as in the feathering of a marine towed streamer, ocean-bottom acquisition, or on-shore acquisition. A numerical example shows that treating the non-horizontal acquisition surface as if it is horizontal can bring severe artifacts to both the attenuation prediction result and the elimination prediction result. We now consider the experiment in which we treat the non-horizontal acquisition surface as if it is horizontal. Figure 4 shows the acquisition and the model of this experiment. The shape of the acquisition can be described by the function $z_g = 25 \times cos\left(8\pi \frac{x_g - x_s}{400}\right)$, where z_g is the depth of the receivers, and $x_g - x_s$ is the offset of the receivers. Figure 5 shows the numerical result of the experiment, where artifacts dominate the prediction shot gathers. Even though the multiple events are isolated from the primaries, if we treat a non-horizontal acquisition surface as if it is horizontal, it is not likely to achieve multiple attenuation, let alone multiple elimination. Since the ISS internal multiple attenuation and elimination algorithms work in the pseudo-depth domain, we take a step back and look into $b_1(k,z)$ and try to locate the reason for such artifacts. Figure 6a shows the water speed uncollapsed Stolt migration $(b_1(k,z))$ of the data in figure 3a, which is collected from the horizontal acquisition surface. Figure 6b shows the water-speed uncollapsed Stolt migration of the data in figure 5a, which is collected from the non-horizontal acquisition surface. If we compare the two migration results, for the first event of b_1, instead of spike, we get a wide-spread event if we treat the non-horizontal acquisition surface as if it is horizontal. This is the reason why we are getting so many artifacts in the prediction results. In order to see how the wrong acquisition geometry assumption lead to the artifacts in the result, we need to review the derivation of $b_1(k,z)$ of a 1D earth.

Start from the Green's theorem bilinear form

$$G(x_s,z_s,x_g,z_g,\omega)=\frac{1}{2\pi}\int_{-\infty}^{+\infty}dk_s'\frac{e^{ik_s'(x_g-x_s)}e^{iq_s'|z_g-z_s|}}{2iq_s'} \tag{5}$$

If the depth of the sorce $z_s=0$,

$$G(x_s,z_s=0,x_g,z_g,\omega)=\frac{1}{2\pi}\int_{-\infty}^{+\infty}dk_s'\frac{e^{-ik_s'x_s}}{2iq_s'}e^{ik_s'x_g}e^{iq_s'z_g} \tag{6}$$

This Green's function can be treated as the superposition of the incident plane waves $e^{ik_s'x_g}e^{iq_s'z_g}$ with an exponential weight. According to Nita et al. (2004), for an incident plane wave $e^{ik_s'x_g}e^{iq_s'z_g}$, the reflected wavefield from the first reflector is $R(k_s',q_s')e^{ik_s'x_s}e^{iq_s'(2z_1-z_g)}$, where z_1 is the depth of the first reflector, and R is the reflection coefficient in wavenumber domain. So the reflected data collected by the receivers will be

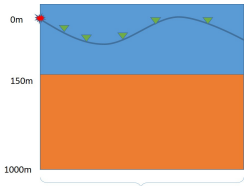

Figure 4: Earth model for the input data with a non-horizontal acquisition

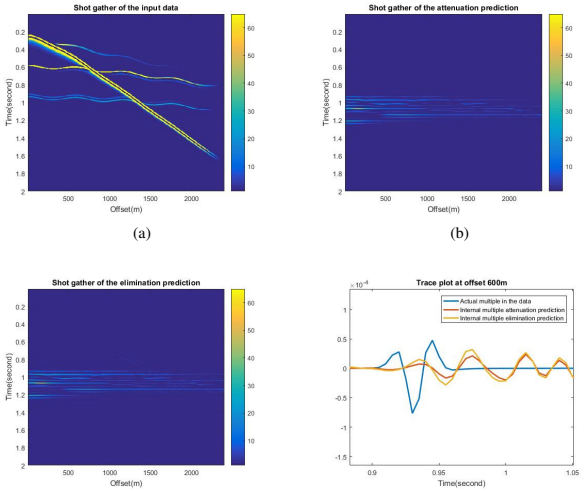

(a) (b) (c) (d)

Figure 5: **(a)** Shot gather of the input data from a non-horizontal acquisition. **(b)** Shot gather of the attenuation prediction using figure 5a as input. **(c)** Shot gather of the elimination prediction using figure 5a as input. **(d)** Trace comparison at offset 600m.

$$D(x_s,z_s=0,x_g,z_g,\omega)=\frac{1}{2\pi}\int_{-\infty}^{+\infty}dk_s'\frac{e^{-ik_s'x_s}}{2iq_s'}R\left(k_s',q_s'\right)e^{ik_s'x_g}e^{iq_s'(2z_1-z_g)} \tag{7}$$

For a 1D earth, the relationship between b_1 and the data D is the following

$$b_1(k,\omega)\;=\;4i\pi q\int_{-\infty}^{+\infty}d(x_g-x_s)\,D(x_s,z_s=0,x_g,z_g=0,\omega)\,e^{-ik(x_g-x_s)} \tag{8}$$

When $z_g=0$, which means the acquisition surface is horizontal, plug in $D(x_s,z_s=0,x_g,z_g,\omega)$, and we have

$$\begin{aligned}b_1(k,\omega)&=q\int_{-\infty}^{+\infty}d(x_g-x_s)\,e^{-ik(x_g-x_s)}\int_{-\infty}^{+\infty}dk_s'\frac{R}{q_s'}e^{ik_s'(x_g-x_s)}e^{iq_s'\left(2z_1-z_g\right)}\\&=q\int_{-\infty}^{+\infty}dk_s'\frac{R}{q_s'}e^{iq_s'2z_1}\int_{-\infty}^{+\infty}d(x_g-x_s)\,e^{i\left(k_s'-k\right)(x_g-x_s)}\\&=q\int_{-\infty}^{+\infty}dk_s'\frac{R}{q_s'}e^{iq_s'2z_1}\,\delta\left(k_s'-k\right)\\&=Re^{i\cdot2q\cdot z_1}\end{aligned} \tag{9}$$

Fourier transform $b_1(k,\omega)$ with respect to $2q$, and we have

$$b_1(k,z)=\frac{1}{2\pi}\int_{-\infty}^{+\infty}d(2q)\,e^{-i\cdot2q\cdot z}Re^{i\cdot2q\cdot z_1}=R\cdot\delta(z-z_1) \tag{10}$$

When the acquisition is horizontal, the water-speed uncollapsed Stolt migration gives the correct migration result of the first primary, a Dirac delta spike at the correct location of the first reflector z_1 with its reflection coefficient (figure 6a). This delta-like migration result for the first primary in b_1 will interact with the correct migrations of other events and give the correct multiple prediction.

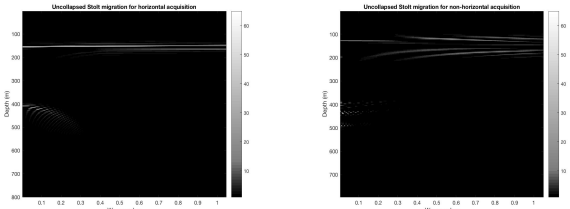

(a) (b)

Figure 6: **(a)** $b_1(k,z)$ for the horizontal acquisition. **(b)** $b_1(k,z)$ for the non-horizontal acquisition

If the acquisition surface is not a horizontal surface, $z_g\neq0$. The depth of the acquisition surface becomes a function of offset $z_g=z_g(x_g-x_s)$. In equation 9, z_g can no longer be left out. $b_1(k,\omega)$ becomes the following

$$\begin{aligned}b_1(k,\omega)&=q\int_{-\infty}^{+\infty}dk_s'\frac{R}{q_s'}e^{iq_s'2z_1}\int_{-\infty}^{+\infty}d(x_g-x_s)\,e^{i\left(k_s'-k\right)(x_g-x_s)}\cdot e^{-iq_s'z_g}\\&=\tilde{I}(k,\omega,z_1)\end{aligned} \tag{11}$$

Fourier transform $b_1(k,\omega)$ with respect to $2q$, we have

$$\begin{aligned}b_1(k,z)&=\frac{1}{2\pi}\int_{-\infty}^{+\infty}d(2q)\,b_1(k,\omega)\,e^{-i\cdot2q\cdot z}\\&=\frac{1}{2\pi}\int_{-\infty}^{+\infty}d(2q)\,\tilde{I}(k,\omega,z_1)\,e^{-i\cdot2q\cdot z}\\&=I(k,z,z_1)\end{aligned} \tag{12}$$

Instead of a delta spike-like function, $b_1(k,z)$ becomes some kind of function I whose form depends on the shape of the acquisition surface $z_g(x_g-x_s)$. Hence $b_1(k,z)$ is not the correct migration result of the first primary. Since the ISS internal multiple attenuation and elimination algorithms work in the psudo-depth domain by combining the migration result of different sub-events (primaries), the ISS internal multiple algorithm will not give the correct results when the acquisition surface is not horizontal.

THE GREEN'S THEOREM WAVE-FIELD PREDICTION

In order to fix the artifacts due to the non-horizontal acquisition, we use the Green's theorem wave-field prediction method to predict

a new dataset collected by a horizontal acquisition which locates above the original non-horizontal acquisition, before applying the ISS internal multiple attenuation and elimination algorithms. The method is discussed in detail in Weglein et al. (2011). Consider the following form of Green's theorem equation

$$P(x,z,\omega) = \int_{m.s.} \left\{ P(x',z',\omega) \frac{\partial}{\partial n'} G_0^+(x,z,x',z',\omega) - G_0^+(x,z,x',z',\omega) \frac{\partial}{\partial n'} P(x',z',\omega) \right\} \cdot d\vec{S}' \quad (13)$$

Equation 13 integrates the data along the actual acquisition (horizontal or non-horizontal) and predicts the data collected at a shallower depth z. If we apply the equation to the scenario shown by Figure 4, we can predict a new dataset collected by a shallower horizontal acquisition from the original non-horizontal acquisition surface, shown in figure 7. The corresponding datasets are shown in figure 8a and 8b, for the non-horizontal acquisition and predicted horizontal acquistion, respectively. We then use the predicted dataset as the input of the ISS internal multiple attenuation and elimination algorithms.

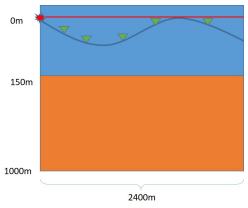

Figure 7: Green's theorem predicts the data from the original non-horizontal acquisition surface (black line) to the new horizontal acquisition surface (red line) above the original one.

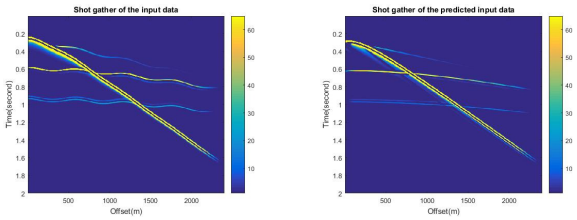

(a) (b)

Figure 8: **(a)** Shot gather of the data from the non-horizontal acquisition. **(b)** Shot gather of the predicted data using Green's theorem wave-field prediction.

NUMERICAL RESULT OF THE ISS INTERNAL MULTIPLE ALGORITHMS AFTER FIXING THE ACQUISITION

In this section we will show the numerical experiment and result of applying Green's theorem wave-field prediction to modify the acquisition before applying the ISS internal multiple attenuation and elimination algorithms. Figure 9a, 9b, 9c shows the predicted horizontal input data, internal multiple attenuation prediction using figure 9a as the input, and the corresponding elimination prediction, respectively. Figure 9d shows the trace comparison at offset 600m of the input data (blue), the attenuation prediction (red), and the elimination prediction (yellow), focusing on the internal multiple part. We can see that, after using the wave-field prediction to fix the shape of the acquisition, the severe artifact disappears in both the attenuation and elimination prediction results.

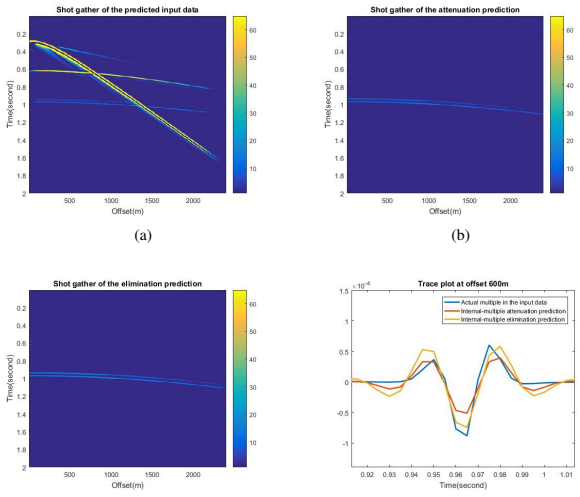

(a) (b) (c) (d)

Figure 9: **(a)** Shot gather of the predicted input data. **(b)** Shot gather of the attenuation prediction using figure 8b as input. **(c)** Shot gather of the elimination prediction using figure 8b as input. **(d)** Trace comparison at offset 600m.

CONCLUSION

The ISS internal multiple attenuation and elimination algorithms have their stand-alone strength since the methods do not need subsurface information. When the multiples are interfering with the target primaries, and the energy-minimization adaptive subtraction might fail, the ISS internal multiple elimination algorithm can still remove the multiples since the algorithm can predict the correct time and amplitude of the multiples. However, the methods have interest and need for a description of the experiment and the acquisition surface. In this paper, we show the necessity of the knowledge of the acquisition surface, examine the impact of the geometry of the acquisition surface on both ISS internal multiple attenuation and elimination algorithms, and we propose to use the Green's theorem wave-field prediction method to fix the artifact in the ISS algorithms due to the wrong assumption of the acquisition geometry. By combining the Green's theorem wave-field prediction and the ISS internal multiple algorithms, we extend the stand-alone capability of the ISS internal multiple algorithms to the non-horizontal acquisitions.

ACKNOWLEDGMENTS

We would like to thank the M-OSRP sponsors for their support. We would also like to thank all M-OSRP members, especially Yanglei Zou and Dr. Mayhan, for their valuable comments and suggestions.

REFERENCES

Araujo, F. V., A. B. Weglein, P. M. Carvalho, and R. H. Stolt, 1994, Inverse scattering series for multiple attenuation: An example with surface and internal multiples: 64th Annual International Meeting, SEG, Expanded Abstracts, 10391041, http://dx.doi.org/10.1190/1.1822691.

Nita, B.G., K. H. Matson, and A. B. Weglein, 2004, Forward scattering series and seismic events: Far field approximations, critical and postcritical events. SIAM Journal on Applied Mathematics, 64(6), pp.2167-2185.

Weglein, A. B., F. A. Gasparotto, P. M. Carvalho, and R. H. Stolt, 1997, An inverse-scattering series method for attenuating multiples in seismic reflection data: Geophysics, 62, 19751989, http://dx.doi.org/10.1190/1.1444298.

Weglein, A. B., F. V. Araujo, P. M. Carvalho, R. H. Stolt, K. H. Matson, R. T. Coates, D. Corrigan, D. J. Foster, S. A. Shaw, and H. Zhang, 2003, Inverse scattering series and seismic exploration: Inverse Problems, R27R83.

Weglein, A.B., R. H. Stolt, and J. D. Mayhan, 2011, Reverse-time migration and Green's theorem: Part I – The evolution of concepts, and setting the stage for the new RTM method. Journal of Seismic Exploration, 20(1), p.73.

Zou, Y., C. Ma. and A. B. Weglein, 2016, The first inverse-scattering-series internal multiple elimination method for a multidimensional subsurface. In SEG Technical Program Expanded Abstracts 2016 (pp. 4550-4554). Society of Exploration Geophysicists.

Zou, Y., and A. B. Weglein, 2014, An internal-multiple elimination algorithm for all reflectors for 1d earth, Part I: Strengths and limitations: Journal of Seismic Exploration, 23, 393404.